

Performance of Genomic Bordering Elements at Predefined Genomic Loci

Sandra Goetze,[†] Alexandra Baer,[‡] Silke Winkelmann, Kristina Nehlsen,
Jost Seibler,[§] Karin Maass, and Jürgen Bode*

German Research Centre for Biotechnology (GBF), Braunschweig, Germany

Received 23 June 2004/Returned for modification 19 August 2004/Accepted 6 December 2004

Eukaryotic DNA is organized into chromatin domains that regulate gene expression and chromosome behavior. Insulators and/or scaffold-matrix attachment regions (S/MARs) mark the boundaries of these chromatin domains where they delimit enhancing and silencing effects from the outside. By recombinase-mediated cassette exchange (RMCE), we were able to compare these two types of bordering elements at a number of predefined genomic loci. Flanking an expression vector with either S/MARs or two copies of the non-S/MAR chicken hypersensitive site 4 insulator demonstrates that while these borders confer related expression characteristics at most loci, their effect on chromatin organization is clearly distinct. Our results suggest that the activity of bordering elements is most pronounced for the abundant class of loci with a low but negligible expression potential in the case of highly expressed sites. By the RMCE procedure, we demonstrate that expression parameters are not due to a potential targeting action of bordering elements, in the sense that a linked transgene is directed into a special class of loci. Instead, we can relate the observed transcriptional augmentation phenomena to their function as genomic insulators.

Bordering or insulator activities protect genes within a chromatin domain from stimulatory and repressive effects arising from flanking genomic regions (8). Several elements implicated in bordering functions have been characterized, among these the scaffold-matrix attachment regions (S/MARs) and insulators (2).

S/MARs were discovered 2 decades ago, when they were first defined as DNA elements that either remain at the nuclear skeleton after the extraction of histones and other soluble factors in a halo-mapping approach (36) or reassociate with a scaffold or matrix preparation with high affinity *in vitro*. The latter procedure was pioneered by Cockerill and Garrard (14). To date, several variants of this protocol are available, permitting the precise quantification of the interaction strength (24, 31), which is a parameter that lends itself to computer-assisted predictions (7). Subsequently, domain-bordering activities as well as multiple S/MAR-enhancer interactions (both negative and supportive) have been reported; the latter class of activities is outside the scope of this contribution.

Recent halo fluorescence *in situ* hybridization (halo-FISH) studies confirm that S/MARs act by organizing eukaryotic chromatin into separate loops (27). Following histone extraction, these loops can be visualized as a DNA halo anchored to the densely stained nuclear matrix or chromosomal scaffold (23, 25). At a molecular level, S/MAR elements interact with constitutive proteins like the abundant scaffold attachment fac-

tor SAF-A (otherwise known as hnRNP U) (26) or lamins, but these contacts can become subject to regulation by cell-type-specific factors (9, 15, 33). The establishment of independently regulated domains by loop formation constitutes a simple but stringent mechanism for chromatin insulation. However, there is no direct evidence yet that this mode of action is shared by all boundary elements or that it holds in every chromosomal context.

Insulators have been mostly defined as sequences that prevent enhancers from inappropriately activating the promoter of an unrelated gene. This positional enhancer-blocking function was first described for *Drosophila melanogaster* but has subsequently also been detected in vertebrates, where it correlates with the association of the CCCTC-binding factor CTCF (6, 48). Prominent elements of this type have been found at the ends of the open chromatin domain in the chicken β -globin locus (chicken hypersensitive site 4 [cHS4]) and within the β -globin loci of humans and mice. A second feature common to some but not all insulators is their ability to protect a transgene from position effects (bordering function). When genes are removed from their native context, dominant influences of a new chromosomal environment become effective leading to aberrant expression characteristics. Influences of this sort become obvious in the common case of a reporter gene integrating in a region of condensed, inactive chromatin (18) or (in rare cases) next to an endogenous enhancer.

Apparently, there is no unique mechanism to explain the performance of domain borders. They may regulate gene expression by controlling the subnuclear organization of DNA, as in *Saccharomyces cerevisiae*, where clustering of binding sites to elements of the nuclear architecture has been correlated with barrier functions (30). This was also illustrated for the gypsy insulator of *Drosophila*, which causes DNA to move either to the nuclear periphery (22) or to sites in the nuclear interior (49). CTCF, on the other hand, associates with the cHS4 in-

* Corresponding author. Mailing address: German Research Centre for Biotechnology (GBF), RDIF/Epigenetic Regulation, Mascheroder Weg 1, 38124 Braunschweig, Germany. Phone: 49 (531) 6181-251. Fax: 49 (531) 6181-262. E-mail: jbo@gbf.de.

[†] Present address: Swammerdam Institute for Life Sciences, University of Amsterdam (UvA), 1098 EL Amsterdam, The Netherlands.

[‡] Present address: Symphogen A/S, 2800 Lyngby, Denmark.

[§] Present address: ARTEMIS Pharmaceuticals GmbH, 51063 Cologne, Germany.

sulator, which in turn becomes tethered to the surface of nucleoli via nucleophosmin (51).

Site-specific recombination has become a powerful tool for the targeted integration of transgenes into predefined chromosomal loci. The technique has been successfully applied both to achieve a predictable gene expression in cell culture (5) and for the systematic generation of transgenic animals (12). Here, we used recombinase-mediated cassette exchange (RMCE) (5) to study the effect of different types of putative domain boundaries at five genomic loci in murine cells. Using halo-FISH, we illuminated aspects of chromatin organization of the targeted locus. Our results indicate that insulating activities of bordering elements depend both on the kind of boundaries and on the genomic context.

MATERIALS AND METHODS

Plasmids. Construction of the plasmid F3hygtkF followed the procedure described previously, using the F3 spacer sequence TTCAAATA in combination with the F sequence TCTAGAAA (42). The *hygtk* gene in F3hygtkF is driven by the herpes simplex virus (HSV)-*tk* promoter. For the exchange constructs an SLG expression cassette containing a luciferase-enhanced green fluorescent protein (eGFP) fusion protein under the control of the simian virus 40 (SV40) enhancer-promoter was used (see Fig. 3A). The luciferase-eGFP fusion gene was flanked by different bordering elements (F3LSLGLF, F3HSLGHF, F3ESLGF, and F3ISLGLF).

Cell culture and gene transfer. NIH 3T3 cells were cultured in Dulbecco's modified Eagle's medium containing 10% fetal calf serum, 20 mM glutamine, 60 μ g of penicillin/ml, and 100 μ g of streptomycin/ml. CHO cells, which were used for excision experiments, were cultured in Nut.Mix F12 (HAM) medium with GlutaMAX (Gibco) which was supplemented with 19% fetal calf serum, 60 μ g of penicillin/ml, and 100 μ g of streptomycin/ml.

Electroporation. Logarithmically growing semiconfluent cells were trypsinized and washed with 1 \times phosphate-buffered saline (PBS). The cells were collected by centrifugation (400 \times g; 5 min). The cellular pellet was resuspended in 500 μ l of electroporation buffer (20 mM HEPES [pH 7.05], 137 mM NaCl, 5 mM KCl, 7 mM sodium phosphate, 6 mM dextrose) containing 2 μ g of linearized DNA.

Transfection. Exchange plasmids were transferred by CaCl₂ transfection. DNA precipitates were prepared as follows: 8 μ g of the supercoiled exchange plasmid and 12 μ g of the FLPe-Puro exchange plasmid were dissolved in 500 μ l of 250 mM CaCl₂ and added dropwise to 500 μ l of 2 \times HeBS buffer (50 mM HEPES [pH 7.1], 280 mM NaCl, 1.5 mM Na₂HPO₄).

Selection for RMCE. The parental NIH clones were cultured with either 200 U (N15/N40/N33) or 500 U (N7/N1) of hygromycin prior to transfection to prevent spontaneous deletions. For an RMCE reaction mixture, 3E5 cells were seeded on a medium-sized plate. After 24 h, 8 μ g of the exchange plasmid was cotransferred with 12 μ g of a recombinase expression plasmid containing a puromycin resistance gene (45). Positive selection with 2.5 μ g of puromycin/ml was applied on day 2 to 3. On day 3, cells were sorted for eGFP expression, seeded at low densities (10⁴ cells per 100 mm) and cultured in the presence of 10 μ M ganciclovir. Clones were isolated on day 11. Exchange events were finally confirmed by Southern blot analysis (4).

β -Galactosidase reporter assay (MUG assay). The β -galactosidase (β -Gal) reporter assay was carried out as described previously (25). In short, the activity of β -Gal in cell lysates was determined via the hydrolysis of the β -Gal substrate 4-methylumbelliferyl D-galactoside (MUG). Fluorescence was determined at 5-min intervals with a Wallace Victor multiple-counter plate reader with excitation at 365 nm and emission at 450 nm. Readings for each sample were determined in triplicate, corrected for the cell number, and referred to a known concentration of purified β -Gal (Sigma).

Luciferase assay. A total of 10⁵ and 10⁶ cells were lysed by consecutive freezing and thawing in 250 mM Tris-HCl (pH 7.5). A total of 20 μ l of the extracts was added to 350 μ l of reaction buffer (25 mM glycylglycine [pH 7.8], 5 mM ATP, 15 mM MgSO₄) and immediately measured with 100 μ l of luciferin solution (0.2 mM luciferin in 25 mM glycylglycine [pH 7.8]).

Quantification of S/MAR activities in vitro (halo reassociation). In vitro-binding assays of DNA sequences to lithium salt (LIS)-extracted nuclear matrices were carried out and quantified according to the modified equal counts approach as previously described (24, 31). This procedure includes a stringent control of the scaffold-binding potential.

Halo preparation. For preparation of nuclear halos, cells were harvested by trypsinization, centrifuged at 200 \times g for 2 min, and stored at -70°C in FSB (50 mM HEPES, 10 mM NaCl, 5 mM Mg acetate [pH 7.5], and 25% glycerol). For the extraction procedure, cells were thawed, washed twice with PBS, and incubated on ice with CSK buffer [10 mM piperazine-N,N'-bis(2-ethanesulfonic acid) (PIPES), 100 mM NaCl, 0.3 M sucrose, 30 mM MgCl₂, 1% Triton X-100] for 15 min. Isolated nuclei were counted, and 1.8 \times 10⁴/50 μ l were pelleted onto slides with a Cytospin centrifuge (800 rpm; 5 min). Slides were treated with 2 M NaCl buffer (2 M NaCl, 10 mM PIPES [pH 6.8]), 10 mM EDTA, 0.1% digitonin, 0.05 mM spermine, and 0.125 mM spermidine) for 2 min to extract soluble proteins. They were then subjected to a series of 10 \times , 5 \times , 2 \times , and 1 \times PBS washes, followed by a series of rinses at 70, 90, and 100% ethanol concentrations. Slides were air dried and baked for fixation at 60 to 70°C for 2 h.

Immunostaining. Slides were fixed with ice-cold methanol:acetone (1:1) and subsequently permeabilized with PBS containing 0.5% Triton X-100. After an initial blocking step, the slides were incubated with either CTCF or lamin-B primary antibody (Santa Cruz). The slides were washed three times to remove excess antibody with PBS containing 0.2% Tween. The cells were then incubated for 45 min at room temperature with a fluorescein isothiocyanate-labeled goat anti-mouse immunoglobulin G antibody (Jackson). Cells were washed as previously described and finally mounted with Vectashield containing DAPI (4',6'-diamidino-2-phenylindole) (0.187 μ g/ml).

FISH. Integrated transgenes were detected with nick-translated plasmid DNA probes (25). As a control for performance of the halo extraction procedure, the localization of telomeres (at the matrix) and centromeres (in the loops) was monitored as in previous studies (25, 39).

After signal detection, samples were examined with a Zeiss Axiovert 135TV microscope equipped with a 100 \times /1.30 oil Plan Neofluar objective and epifluorescence and filter sets from Omega Optical (Brattleboro, Vt.). Images were acquired with a Photometrics (Tucson, Ariz.) high-resolution, cooled charge-coupled device camera (PXL 1400; grade 2) for 12-bit image collection with IPLab Spectrum custom software from SignalAnalytics. This software includes a coloring of black-and-white pictures taken at different wavelengths and a subsequent overlay.

Statistical analysis. To test for significance, a statistical analysis of data from unpaired groups was done by Student's *t* test. A significance level of 0.05 was chosen for all calculations.

RESULTS

Excision of flanking S/MAR elements. S/MAR elements represent a group of noncoding sequences with a regular distribution of AT-rich patches, a criterion that lends itself to computer-assisted prediction by the SIDD (stress-induced duplex destabilization) algorithm (7) and which has been shown to be more important than the overall A+T content (47). S/MAR sequences are bound by specialized protein complexes within the eukaryotic nucleus, commonly designated nuclear matrix proteins (10). To appreciate the activity of S/MARs at the borders of a putative minidomain, we performed a pilot experiment in which we created a construct flanked on both ends by the 800-bp core of the well-characterized beta-interferon (IFN- β) upstream 2.2-kb S/MAR element E (for S/MAR-element E, <http://smartdb.bioinf.med.uni-goettingen.de/cgi-bin/SMARTDB/getSMAR.cgi?SM0000002>). Both the extended S/MAR element and the 800-bp core, which contributes most of its activity (7), were originally described by Mielke et al. (35), who designated them I (2.2 kb) and IV (800 bp), respectively.

Core fragment IV has proven its potential to augment transcription levels (1, 35) and to interfere with DNA methylation (3). For the present study, it formed the upstream and the downstream border next to a β -Gal (*lacZ*) reporter (Fig. 1A). Each border was flanked in turn by a pair of identical recombinase target sites, FRT (upstream) or LoxP (downstream), enabling their individual excision by the respective site-specific

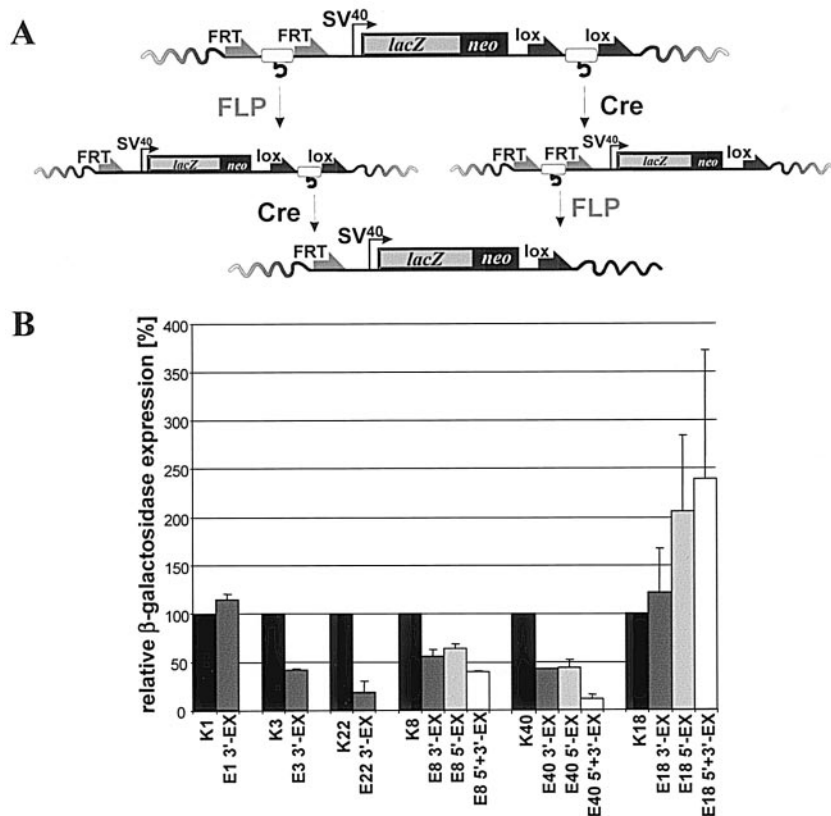


FIG. 1. The excision concept. (A) The presence of flanking FRT or LoxP sites (half arrows) enables the individual excision of bordering S/MAR elements by pulses of Flp or Cre recombinase, respectively. (B) Recombinase transfected cells were selected, the excision event was verified, and the transgene expression rates were determined via a MUG assay. Expression values were normalized to the expression of β -Gal of the full-size construct within the respective locus. For a number of excision clones (designated EX), the loss of bordering S/MARs significantly affected reporter gene expression by exposing it to the surrounding chromatin.

recombinase, Flp or Cre (Fig. 1A) (9). We have shown before that excision reactions of this type proceed to completion, owing to thermodynamic and kinetic forces (29).

Figure 1B illustrates the results of this procedure for six authentic single-copy clones, each with the reporter cassette at a different genomic locus. The results clearly demonstrate that exposure of the reporter to the chromatin environment, i.e., the excision of one or both bordering elements, led to effects that depended to a remarkable extent on the nature of the integration site. While in most cases, excision impaired expression levels, as expected from the overall results of previous standard transfection experiments (41), there were significant exceptions: for clones K1 and K18, excision caused no negative effect (K1) or even a positive effect. Where excision of both borders could be achieved (K18), the effect was additive. All other clones had reduced expression levels after excision; for K8 and K40, this was caused by the removal of either the 3' or the 5' border; if both borders were deleted, an additive influence became apparent again.

These results indicate that S/MARs share at least some properties with prototypical insulators. They also demonstrate that their overall positive effect on transcription levels, i.e., their augmentation potential (8) does not depend on a hypothetical activity such as a targeting element that would direct an S/MAR gene-S/MAR transgene into a class of genomic loci

different from that of the S/MAR-free control. Obviously, it is rather a consequence of shielding the mostly negative influences of the genomic environment (18).

Together with our experience with standard gene transfer techniques, we have to conclude that the effect of bordering elements on the level of transcription significantly depends on the locus of transgene integration. In several series of nontargeted transfection experiments, we have tried to investigate pools of colonies for an initial statistical evaluation of bordering elements at multiple loci. These pilot studies revealed the following properties, which clearly called for improvement. In cases where multiple-copy integration events predominated, we found repeat-induced silencing phenomena (21). In addition, instability was introduced by the repetition of identical sequences. This was particularly evident for double S/MAR constructs, probably due to the recombinogenic character of these elements (8). With an electroporation protocol optimized for the prevalence of single-copy integration events (4), a minidomain containing a GTN (*gfp-tk-neo* resistance) cassette flanked by S/MAR elements E (human IFN- β upstream) and W (<http://smartdb.bioinf.med.uni-goettingen.de/>; see also discussion below) mediated a more homogenous expression than the other domain borders (see Fig. 3A) and no indication of long-term shutoff events. The same element combination

had proven its performance in rodent cells before, underlining the transspecies activity of S/MAR elements (8, 41).

In the following experiment, we exploited an approach to directly compare the performance of authentic single-copy double S/MAR and double cHS4 minidomain constructs at identical genomic loci. Obviously, the excision approach is not suited for a stringent comparison of S/MAR and cHS4 elements, as it represents a one-way road: the reaction usually cannot be reversed to enable integration. This aim, however, is readily achieved by RMCE, as shown in previous studies (5, 9, 12). The procedure leaves behind the expression cassette in the absence of a coexpressed selection gene, preventing artifacts, due to promoter occlusion or related phenomena (28).

Comparing bordering elements with regard to expression properties: the concept. It has been proposed that S/MAR elements, as well as insulators, may counteract the overall repressive effect (18) of chromatin, enabling a stable expression at randomly selected sites of integration. Insulators like cHS4 shield a promoter from the effects of an upstream enhancer and reduce position effects on mini-*white* expression in *Drosophila* cells. The same is true for certain S/MAR elements, which are thought to gain this property by binding to components of the nuclear matrix (2). To directly compare and possibly distinguish the mode of action between these classes of genomic elements, we generated a construct (the parental construct [Fig. 2]) that was integrated into the genome of murine cells as a target. This target could subsequently be addressed by an exchange vector, enabling the replacement of the parental cassette via RMCE. Both the target and the exchange vector had their gene cassettes flanked by the same set of heterospecific F₁-recombinase target sites, i.e., one wild-type site (F) and one spacer mutant (F3). Such a set of sites permitted cassette exchange by a double-reciprocal crossover (F × F and F3 × F3), provided that there was no cross-interaction between the members within a set (i.e., no F × F3 recombination) (9). In the results shown in Fig. 2, the targets were simple cassettes carrying a fusion gene, which encoded a positive (hygromycin) and a negative (HSV-thymidine kinase) resistance marker but no reporter gene. Hyg^r was used to select the recipient cells from which we recovered clones with authentic but different single-copy integration events. To check for the functionality and expression profile of the targeted loci, we used an exchange vector with a *lacZ neo* resistance reporter-selector fusion gene. Successful RMCE events could then be recovered by negative selection, i.e., based on the clone's survival in the presence of ganciclovir (which would be lethal in the continued presence of the *HSV-tk* activity) and on their survival in the presence of G418 (positive selection) as described previously (43). After this procedure, we had the criteria available to select five clones (N15, N40, N33, N7, and N1) with various expression levels to serve as RMCE targets in the experiments that followed.

Flank classes. Compared to the data shown in Fig. 2, the exchange vectors shown in Fig. 3A represented more elaborate cassettes: the SLG transcription unit (a luciferase-eGFP fusion under the control of the SV40 promoter) allows the optional detection of two reporters (luciferase and GFP) for quantification. The transcription unit is further embedded in different classes of flanks, as discussed below.

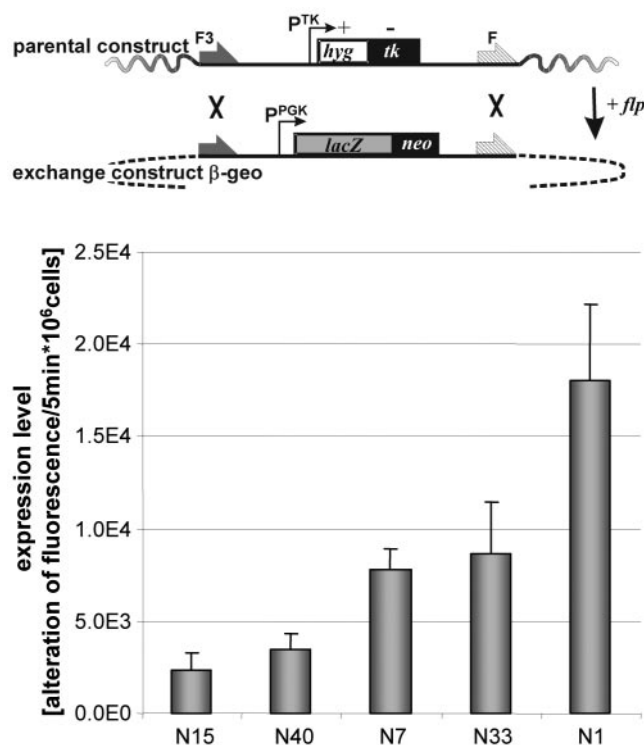


FIG. 2. Level of β -Gal expression in five parental clones established by RMCE. The parental construct containing a *hyg-tk* fusion gene under the control of a *tk* promoter (pTK) is exchanged for a *lacZ-neo* fusion gene cassette that resides on the exchange vector. β -geo is a fusion between the *lacZ* and neomycin resistance genes, yielding a unique reporter-selector protein (20). Exchange clones that have received the β -geo fusion gene by RMCE were expanded in G418 to ensure that all of the cells were expressing the transgene. β -Gal activity in cell lysates was determined via the conversion of MUG. Error bars represent the standard deviation between two genetically identical subclones carrying a β -geo construct. Three separate determinations were performed for each subclone. Statistical analysis revealed a significant difference between average expression levels at loci N15 and N40 in comparison to loci N7 and N33 ($P \leq 6 \times 10^{-3}$) and locus N1 ($P \leq 1 \times 10^{-5}$).

(i) **Two full-length, previously characterized (8, 41) S/MARs.** These S/MARs differ in origin and sequence content, but both have registers of periodically destabilized sites (7). The 2.2-kb element E was described above and was derived from the of the human IFN- β gene. The 1.3-kb element W was from the first intron of the potato leaf stem-specific protein ST-LS1 (<http://smartdb.bioinf.med.uni-goettingen.de/>). This combination of elements has been used before to demonstrate the transspecies activity of S/MARs in a number of transfection assays (8, 41); it has proven long-term stability in both the constitution and expression characteristics of the construct. Both elements have also been used to functionally replace the I γ k chain gene-associated S/MAR with respect to its DNA-demethylating capacity (32).

(ii) **Two novel short S/MAR-type sequences.** These sequences are from an extended intergenic region of the human IFN- α/β gene cluster, i.e., the 567-bp fragment IS20 and the 515-bp fragment IS275, both with an approximately 300-bp-long destabilized core (24); these intergenic insertion elements

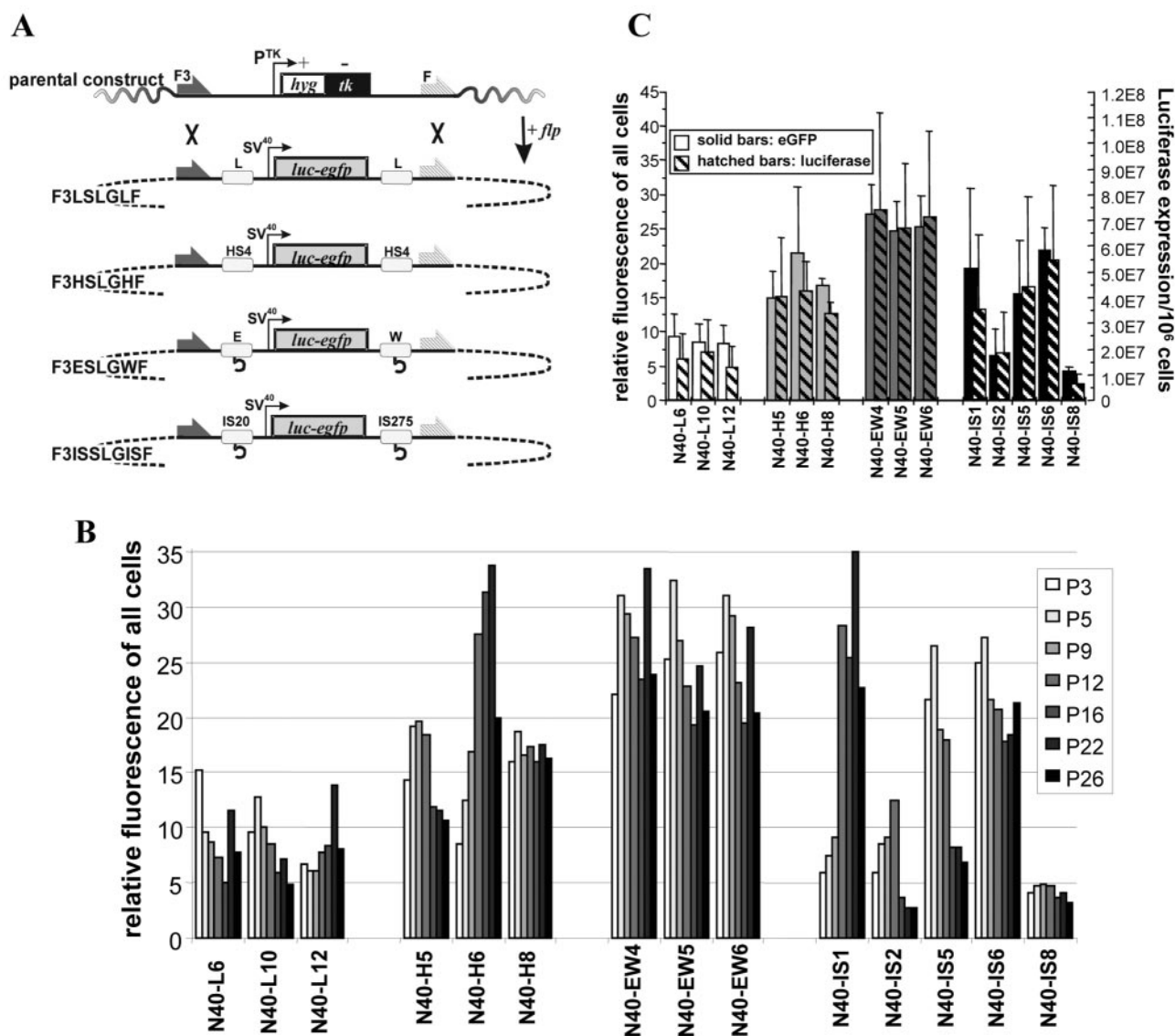


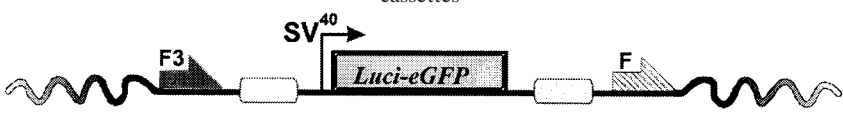
FIG. 3. Effects of boundary elements on expression in the N40 locus. (A) Outline of RMCE reactions. The target vector contains an expression cassette in which the *tk* promoter drives expression of *hyg**tk*, a fusion protein with hygromycin phosphotransferase and thymidine kinase activities; the cassette is flanked by F and F3 elements. The five NIH clones carrying single copies of the parental construct (Fig. 2) were cotransfected with an *flp*-puromycin recombinase expression plasmid and a circular exchange plasmid containing the SV40 promoter driving luciferase-eGFP expression. The desired replacement was selected for by puromycin resistance, FACS, and selection against thymidine kinase expression and finally confirmed by Southern blotting. (B and C) Expression characteristics and stability of subclones derived according to the RMCE approach: expression of eGFP for locus N40 was measured for 26 passages in the absence of selection pressure and evaluated in parallel to luciferase expression (hatched bars in panel C). eGFP expression was quantified by FACS (Fig. 4), and the luciferase assay was performed on cellular extracts as described in Materials and Methods. Both reporter gene acquisition methods correlated well, confirming the expression rates in the different subclone populations. In each of the three subclones, the S/MAR-EW bordering elements caused the highest levels of eGFP and luciferase expression in comparison to other flanking DNA sequences. Between the groups of bordering elements, a significant difference in average transgene expression was observed ($3 \times 10^{-5} \geq P \geq 3 \times 10^{-18}$) except between the insulator (H) and the intergenic (IS) population ($P = 6 \times 10^{-2}$). Error bars are not present in panel B, because data were obtained by a FACS-based population analysis, while panel C summarizes overall expression averages for all passages.

(IS) have been identified by a biomathematical prediction approach (SIDD) and were characterized by competition with prototype S/MARs (24). ISs mediate a strong attachment to both murine and human scaffolds; as prototype S/MARs, they show a strong augmentation effect after stable integration.

(iii) **Two dimers of the *chs4* insulator (H, 2.4 kb).** These dimers are currently regarded as prototype genomic insulators

with transspecies activities regarding both enhancer-blocking and bordering functions.

(iv) **Two supposedly inert spacer sequences.** These sequences are from the λ phage the extensions of which match the above-mentioned prototype S/MARs (L, 2.2 kb and 1.3 kb; see Fig. 8 below). These lambda DNA spacer sequences were placed at either end of a control cassette to exclude a mere distance effect.

TABLE 1. Expression analysis of five genomic loci where the parental construct was exchanged against the different SLG expression cassettes^a


| Locus | Element | | | |
|-------|------------|------------|------------|------------|
| | Lambda | cHS4 | SAR-E/W | IS |
| N15 | 4.1 ± 1.8 | 22.5 ± 7.2 | 8.5 ± 2.0 | 12.6 ± 8.1 |
| N40 | 8.6 ± 0.6 | 17.8 ± 3.3 | 25.7 ± 1.4 | 13.4 ± 7.7 |
| N7 | 18.7 ± 1.6 | 25.6 ± 3.6 | 28.7 ± 2.5 | 17.7 ± 5.2 |
| N33 | 19.2 ± 3.3 | 29.5 ± 6.0 | 22.5 ± 3.2 | 14.1 ± 9.3 |
| N1 | 25.6 ± 0.3 | 29.7 ± 4.5 | 27.2 ± 0.2 | 29.7 ± 0.7 |

^a The relative eGFP fluorescence averaged over all subclones of a given population was measured in the absence of selection pressure for at least 10 passages ± SD. The lambda construct served as a neutral control, reflecting the transcriptional properties of the targeted loci. Dependent on the integration locus itself, the influence of different bordering elements on transgene expression varied greatly. Statistical analysis revealed that there was no significant difference between populations at locus N1; for locus N33, only lambda, SAR-EW, and IS populations were alike. At locus N7, the lambda control differed significantly from the SAR-EW population ($P = 3 \times 10^{-3}$), while at a significance level of $P = 0.05$, no difference between lambda and cHS4 ($P = 6 \times 10^{-2}$) and between lambda and IS ($P = 3.5 \times 10^{-1}$) was detected. At locus N15 as well as at locus N40, average expression levels of all exchange clone populations were clearly different from that of the lambda control.

The two types of S/MARs used in our approach differed with regard to their protein interaction partner at the nuclear matrix: while S/MAR-E and S/MAR-W mainly interacted with the nuclear matrix protein SAF-A (10), the two intergenic attachment elements strongly interacted with a different set of nuclear matrix proteins still to be characterized.

Performance of bordering elements at genomic reference sites and at the single-copy level. For our RMCE approach, we used all five parental clones with a special focus on clone N40, which offered a moderately expressed genomic target (Fig. 2). According to the above results, this locus could be expected to respond to insulation. To monitor expression levels after a successful exchange event, the dual-reporter SLG expression cassette was used, as it allowed eGFP data to be verified by luciferase. Luciferase provides a fast-responding and more-sensitive reporter system, well suited for the detection of low expressers that might arise in the absence of selection pressure. Subclones that had completed RMCE were recovered via eGFP expression and by subsequent negative selection in the presence of ganciclovir. Under these conditions, site-specific recombination was confirmed by Southern blotting, which demonstrated an average targeting efficiency of 20 to 50%.

To assess the effect of clonal variation on the transgene expression rate, several individually established RMCE subclones were cultured in parallel and in the absence of selection pressure. Over 26 passages, eGFP expression status was regularly determined by flow cytometry (Fig. 3B). Figure 3C summarizes the overall expression averages for all passages based on eGFP and luciferase, emphasizing the good correlation between both reporter systems.

Consistent with the characteristics of integration site N40, the relative fluorescence of the lambda expression cassette was moderate with a slight overall decrease in the percentage of expressing cells over time (clones L6, L10, and L12). Placing the cHS4 insulator construct in the same location brought about a clear increase in transgene expression; such an action became even more pronounced when the S/MAR-E and -W elements were used as domain borders (clones H5, H6, and H8). For all S/MAR subclones (EW4, EW5, and EW6), the expression level exceeded that of the control by factors 3 to 4.

Subclones containing the intergenic S/MAR cassette (IS1, IS2, IS5, IS6, and IS8) showed the largest absolute, as well as time-dependent, variation for both eGFP and luciferase expression. Within the populations, there were subclones at the expression level of the lambda control and others that resembled cHS4 (IS6 and IS8). While for the low expresser (IS8), expression patterns remained stable during long-term cultivation, for other clones it showed large time-dependent variations in both the positive (IS1) and the negative (IS5) senses. Like prototype S/MARs, ISs act via an augmentation mechanism: they increase transcription rates in the stable but not the transient expression phase, demonstrating that their action depends on an ordered chromatin structure. But unlike S/MARs and insulators, they do not protect against clonal variation (see also standard deviations for the subclone populations) (Table 1).

In addition to the detailed studies for the N40 locus, we also collected data for the expression of eGFP and luciferase at the other targeted loci. The eGFP expression results have been compiled in Table 1, showing that the noninsulated construct (F3LSLGLF) reflected the properties of the integration locus, as expression levels followed those of the parent constructs (Fig. 2), even in the absence of any selection pressure. These effects were dampened by efficient insulators such as cHS4 and (with the exception of the N15 site) by the EW combination of S/MAR elements. The IS construct shows an intermediate behavior.

The case of the low-expressed locus N15 deserves special attention: in contrast to the N40 locus investigated above for which the S/MAR EW borders resulted in the highest expression levels, this was the case for the cHS4 construct (Fig. 4 and Table 1). When the expression characteristics of clonal cell populations were analyzed by fluorescence-activated cell sorter (FACS) (Fig. 4B), homogenous expression patterns and just small differences were observed for the clones of the H and EW series. This was definitely different for the IS series, where one clone underwent position effect variegation (IS2) and where all clonal populations (IS1, IS2, IS5, and IS11) differed largely in their maximum expression.

Taken together, data from all loci indicate that the cHS4

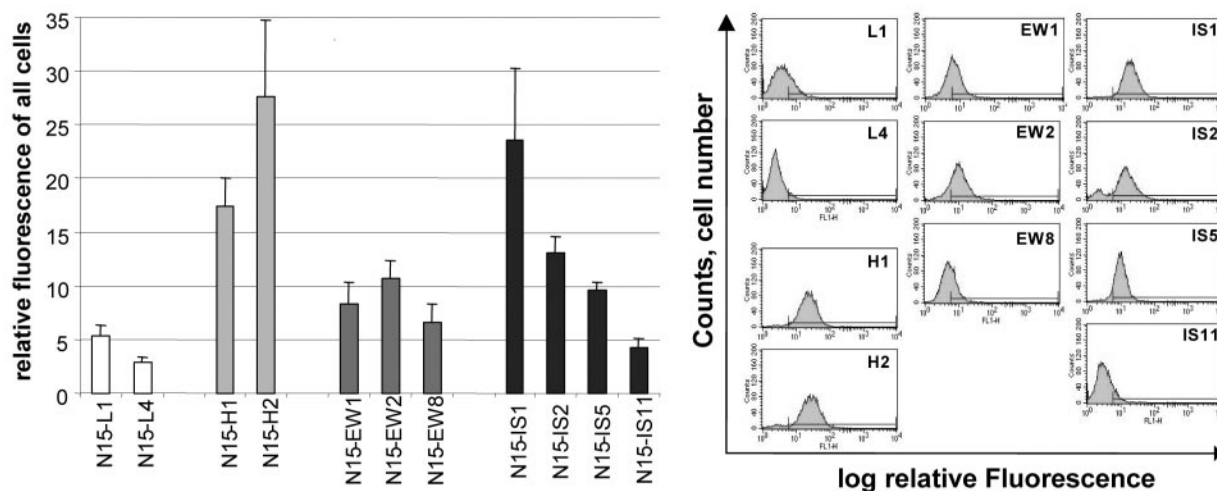


FIG. 4. Flow cytometry analysis for 11 subclones at locus N15. The expression profiles of the individual subclones during 10 passages are summarized in the bar chart. The FACS profile of the same clones at passage 8 shows a uniform distribution of eGFP expression for the S/MAR-EW and cHS4 cassette, while the profile greatly varies between the intergenic subclones (IS); see also Table 1 for a summary of the relative fluorescence of expressing cells (gate M1). *x* axis, log relative fluorescence; *y* axis, cell number.

insulator exerts the strongest shielding function at all loci investigated, although it permits some subclonal variation. Within a given site, however, the EW cassette provides the most uniform expression and shields negative effects from the surroundings of most but not all integration sites.

Classification of bordering elements according to their matrix association status. The RMCE approach has shown that related but nevertheless distinguishable borders of noncoding DNA exert specific effects in a given chromosomal environment. To further characterize their structural function at the molecular level, we performed FISH experiments on nuclear halo preparations by a standardized procedure (25, 27). To this end, nuclei from the individual clones were extracted by high-salt treatment resulting in a DNA halo in which non-matrix-associated DNA was arranged in loops around a proteinaceous network. This network is referred to as an *in situ* nuclear matrix, which attracts S/MAR sequences and actively transcribed genes in a dynamic manner: while active transcription units show some residence at the nuclear matrix, this localization is greatly supported by the presence of S/MARs (27), which assist the transcriptional initiation step (42).

We first evaluated the attachment frequency of the *hyg-*tk** construct at integration site N40. On average, we obtained attachment rates of between 80 to 95%, which indicates integration close to an endogenous S/MAR element. After cassette exchange, the localization of the SLG cassettes was investigated in several of the N40 subclones. For each of these, 50 to 100 single-cell hybridizations were evaluated in at least two independent experiments. The results are summarized in Table 2, and the typical association status of subclones is shown in Fig. 5. The association of the two subclones that are flanked by S/MAR-elements E and W follows our expectations. Also in case of the IS20 and IS275 elements, the association pattern remained largely unaffected by transcription levels, as there was no difference between subclones IS1 to IS8. Even the presence of lambda sequences did not interfere with the chromatin association status in the targeted locus, supporting our

view that the transgene is integrated in a chromatin domain that shows an overall association to the nuclear matrix. However, a striking deviation from this general scheme was observed in the group of cHS4 subclones for which about half of the exchange constructs do not overlap the nuclear matrix. Apparently, introduction of this particular insulator interfered with the chromatin structure of the integration locus. When we subjected the N15 subclones to halo-FISH analysis, we arrived at similar conclusions: chromatin attachment to a high-salt-resistant nuclear matrix did not absolutely reflect the efficiency

TABLE 2. Distribution of SLG expression cassette over loop and matrix portions of a nuclear halo^a

| Locus-subclone | No. of events (signal) | |
|----------------|------------------------|---------------------------------|
| | Total | Nuclear matrix (%) ^b |
| N40 (parental) | 74 | 81 |
| N40-L10 | 52 | 85 |
| N40-L12 | 64 | 81 |
| N40-H5 | 71 | 51 |
| N40-H6 | 53 | 55 |
| N40-EW4 | 62 | 78 |
| N40-EW5 | 66 | 86 |
| N40-IS1 | 82 | 71 |
| N40-IS2 | 183 | 77 |
| N15 (parental) | 79 | 83 |
| N15-L4 | 54 | 84 |
| N15-H2 | 96 | 70 |
| N15-EW1 | 91 | 93 |
| N15-IS2 | 50 | 94 |

^a The genuine distribution values of targeted loci N40 and N15 are seen in comparison to different exchange clones (see Fig. 5). For the N40 insulator clones H5 and H6 and the N15 insulator clone H2, a significant decrease in matrix localization was detected, especially in comparison to the S/MAR constructs. This became even more evident when a surface correction approach for the halo portion covering the nuclear matrix was applied (25). Such a surface correction resulted in minimum matrix attachment values of between 33 and 47%, respectively.

^b Boldface indicates subclones with cHS4 elements.

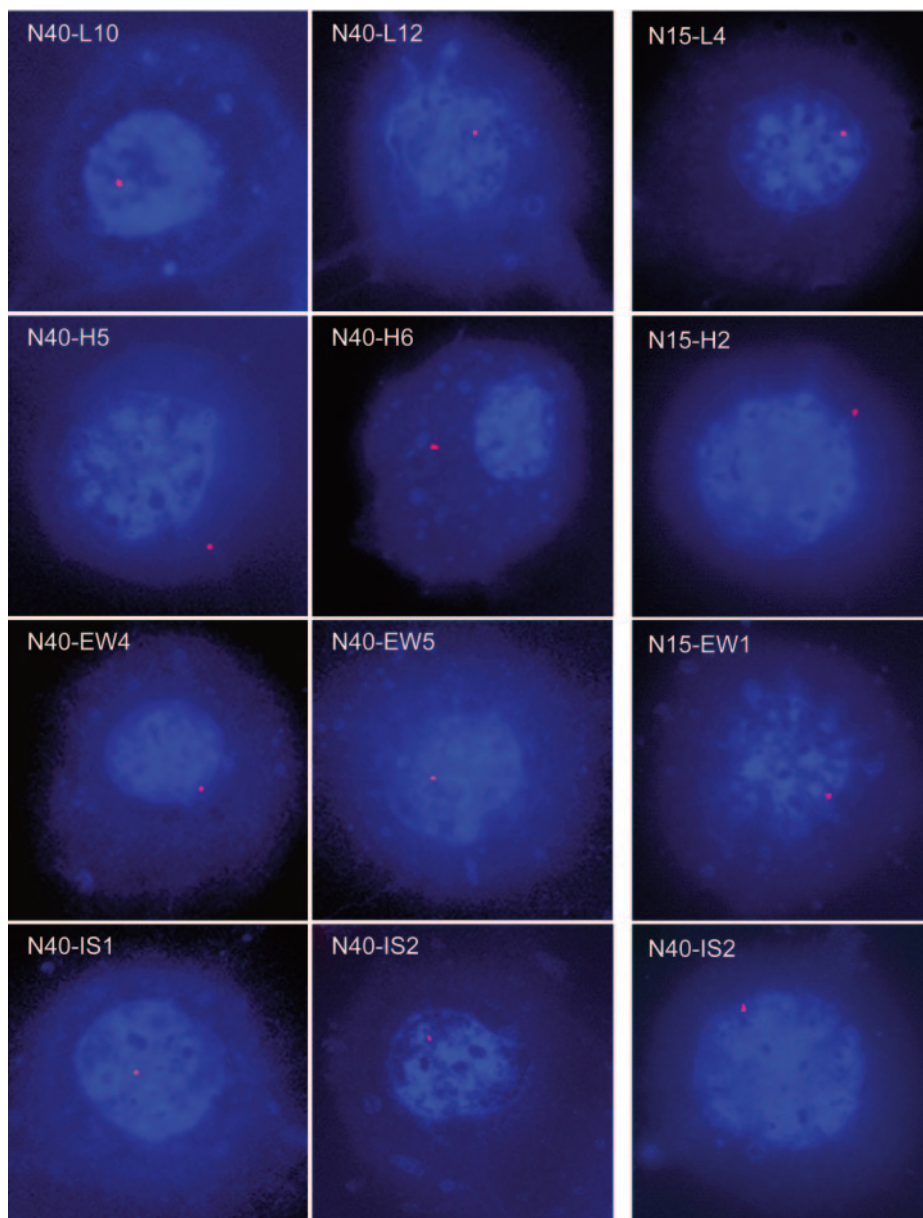


FIG. 5. Distribution of the SLG expression cassette in exchange clones after 2 M NaCl treatment (halo preparation) and FISH. Isolated nuclei from different subclones of N40 and N15 were spun onto slides and extracted with 2 M NaCl to evaluate the localization of the expression cassette with regard to the nuclear matrix. The high-salt treatment led to an extraction of histones and soluble non-matrix proteins, leaving the DNA in loops attached to the residual nuclear matrix (25). The red signal indicates the integrated transgene. Subclones of each exchange population were evaluated. While the integrated lambda, S/MAR-EW, or IS-S/MAR cassette does not significantly alter the organization of the integration locus with regard to the nuclear matrix, the integration of the cHS4 construct led to a partial release of the locus (see also Table 2).

of transgene transcription and, in the case of cHS4 sequences, an alternative mechanism appeared to be active. It is notable that CTCF was recently reported to be part of the nuclear matrix (16). When we immunostained our halo preparations, however, only a very few CTCF foci remained visible in isolated extracted nuclei (Fig. 6); these showed an apparent association with the nucleoli.

The binding affinity of the cHS4 dimer to LIS-prepared nuclear matrices is in line with these observations. Figure 7 demonstrates a quantitative binding assay according to our standardized procedure (31). As a positive control, the strongly

(95%) binding S/MAR-E element was used, whereas the pTZ18R vector backbone served as the negative control. Clearly, no binding (<3%) of the cHS4 dimer to the nuclear matrix could be detected, in accord with a frequently cited previous report (13).

Classification of bordering elements by biomathematical algorithms. The relation between S/MARs and insulators has remained a matter of contention. As for S/MARs, the best insulating capacity arises when a pair of nonidentical elements flanks the gene of interest to yield a minidomain. In such a case, interactions with specific insulator-binding proteins lead

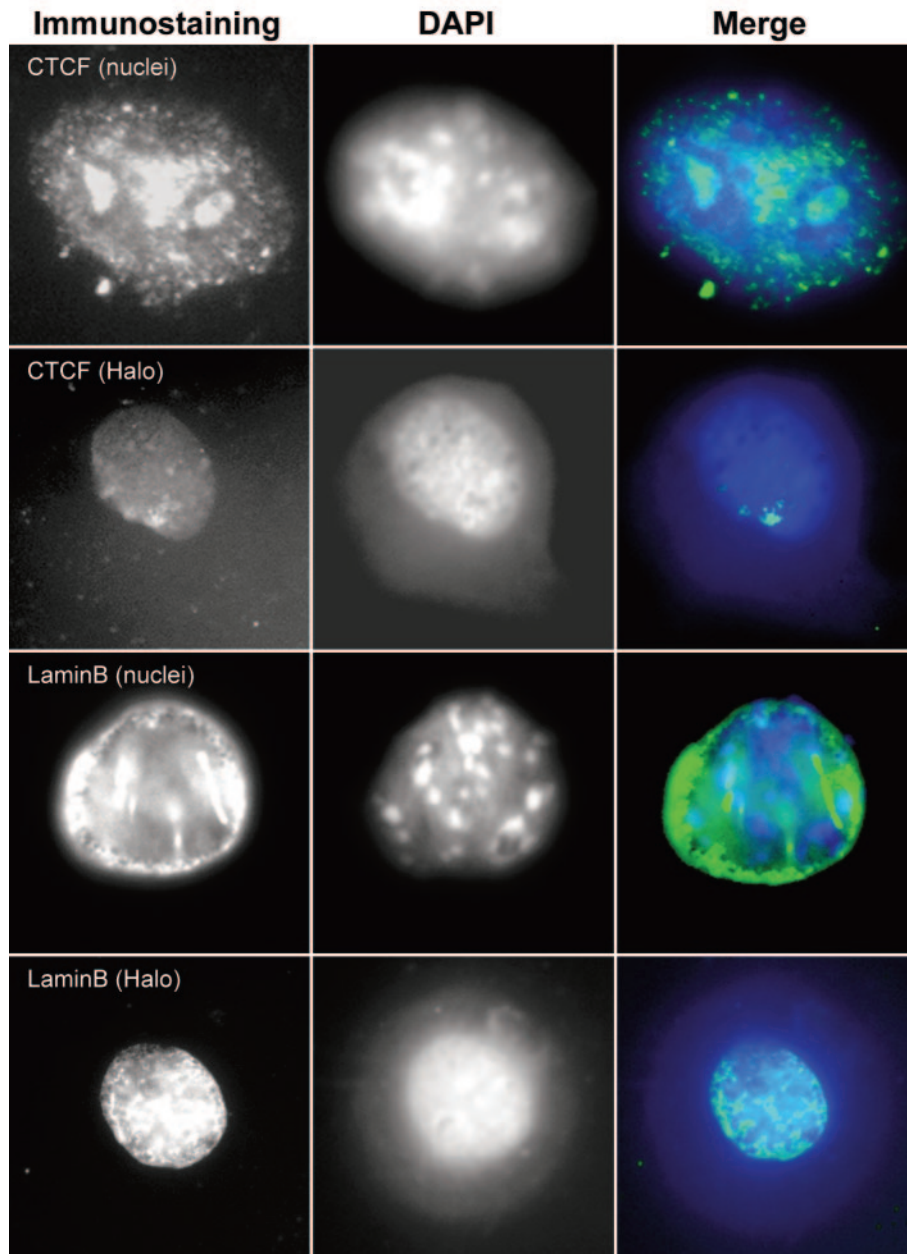


FIG. 6. Lamin-B and CTCF staining in unextracted nuclei and halo preparations. While the lamina is continuously stained by a lamin-B antibody after a 2 M NaCl extraction step (green rim), most of the CTCF was extracted from the nuclear matrix in the DNA halo (green dots). In unextracted nuclei, CTCF was mainly found within the nucleoli.

to a structure reminiscent of the loops that are formed by nuclear matrix attachment (17, 51).

In the following experiment, we applied two common biomathematical algorithms which have been developed as tools to predict S/MARs. The first approach was based on the MAR-Wiz (<http://www.futuresoft.org/MarFinder/>), which relies on the statistical occurrence of S/MAR motifs (44). Alternatively, a statistical mechanical procedure was applied to derive SIDD profiles that identify regions of DNA unwinding and, thereby, secondary-structure-forming potentials (7). There are many cases where the prediction of these two approaches is in close agreement (24).

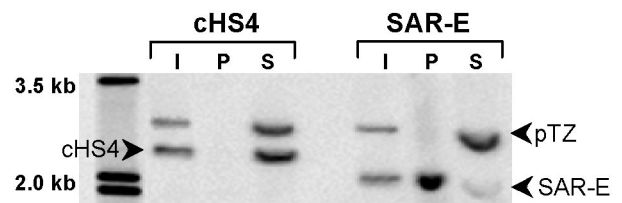


FIG. 7. Affinity of the cHS4 insulator to LIS-extracted nuclear matrices. The *in vitro* S/MAR reassociation assay with a [³⁵S]ATP-labeled 2.4-kb cHS4 sequence shows no affinity of the insulator to the nuclear matrix. As a positive control, the 95% binding S/MAR-E sequence was used, and the pTZ-vector backbone served as negative control. I, input; P, pellet fraction; S, supernatant.

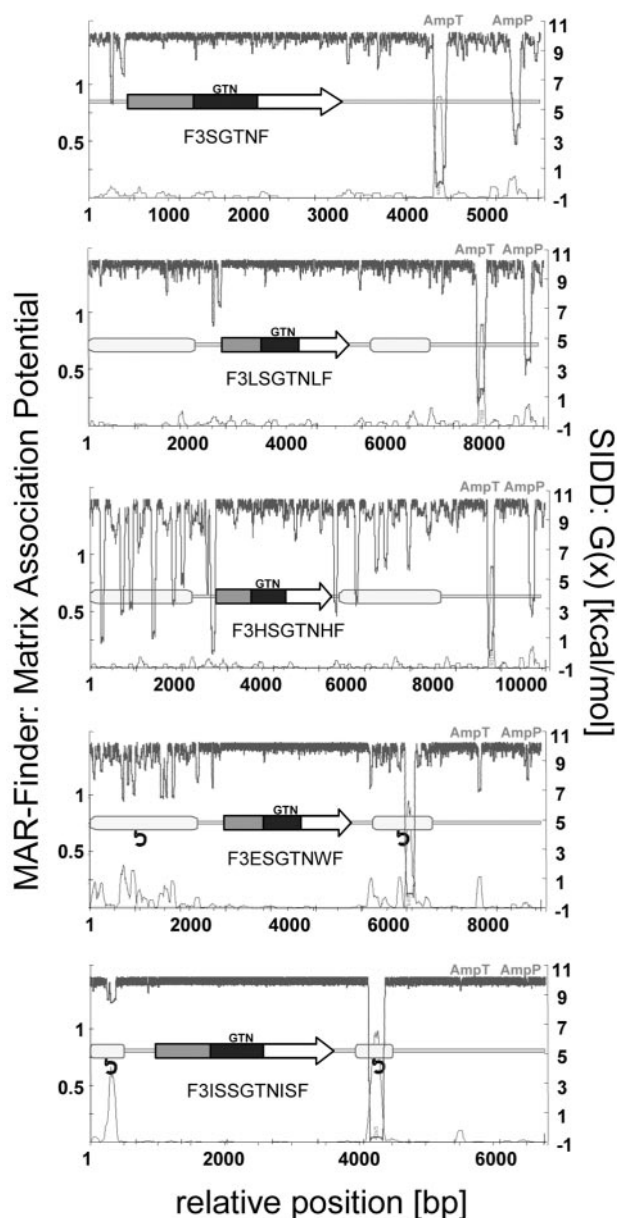


FIG. 8. SIDD and MAR-Wiz profiles for different bordering sequences. The SIDD profile (curve at top of each profile) plots the probability of base unpairing as a function of base pair position in a given sequence stretch. The incremental energy, $G(x)$, reflects the stability of a DNA sequence at a fixed superhelical density ($\sigma = -0.055$) and thereby indicates its tendency to form single-stranded DNA stretches. This feature coincides with the nuclear matrix-binding potential of DNA as described in the text and in reference 7. The MAR-Wiz routine (plot at bottom of each profile) was operated with its default settings (Ori rule, TG richness rule, curved-DNA rule, kinked-DNA rule, Topo II recognition rule, AT richness). This combined theoretical approach underlines the existence of different classes of bordering elements (boxes), especially with regard to S/MAR elements and the cHS4 insulator. AmpT/P, ampicillin promoter-terminator; GTN, *eGFP-tk-neo* fusion gene.

We have previously shown that all S/MARs represent base-unpairing regions that undergo strand separation under the negative superhelicity of a plasmid (superhelix density of $\sigma = -0.055$). For comparative purposes, we analyzed all bordering sequences in the F3SGTNF vector backbone, which in addition to an *eGFP-tk-neo* expression cassette contains the destabilized sites adjacent to the ampicillin resistance gene (AmpT and AmpP) as internal destabilization standards (Fig. 8) (34). Neither of these prokaryotic unpairing elements has any S/MAR activity, but they respond to the amount of destabilization at other regions in the same vector with which they are in competition (7). Prototypical extremes are constructs F3SGTNF and F3LSGTNLF, where the AmpT- and AmpP-related signals are prominent, owing to the lack of other competing sites, and F3ISSGTNIS, where they vanish due to the fact that the IS elements (mostly the downstream element IS275) accommodate superhelical strain, owing to their unwinding potential. Two types of S/MARs are present in construct F3ESGTNWF: whereas a site in S/MAR W is the major unpairing element in this region, S/MAR E consists of a succession of many evenly spaced sites with a reduced individual unpairing potential (7).

For our construct F3HSGTNHF, the predictions are ambiguous. While MAR-Wiz did not uncover any S/MAR-related features in this overall GC-rich element, the SIDD profile reflected a regular distribution of unpairing elements comparable to the S/MAR E in the F3ESGTNWF construct. However, when tested in reassociation experiments (Fig. 7), the cHS4 insulator had no affinity to the nuclear matrix, confirming our conclusion that stress-induced destabilization is a necessary but not sufficient criterion for nuclear matrix attachment potential.

DISCUSSION

The mammalian genome is organized into independently regulated chromatin domains, which support or repress gene expression. The boundaries between these domains are associated with structural elements known as either S/MARs or insulators; there are recent examples where both functions overlap (2, 37). It is common to consider S/MARs a special group of *cis*-acting elements that augment transcription initiation rates by actions different from those of an enhancer (42). Possible mechanisms could involve the targeting of transgenes to particular genomic sites or insulator-like functions. Regarding the dominant influence of chromatin surroundings on the expression of test constructs, a stringent comparison of this type of effects requires integration at the same predefined genomic site. With the advent of RMCE techniques, such an approach has become feasible (5).

Bordering elements and targeting function. In the present study, we compared a double insulator construct with two different double S/MAR constructs at five predefined genomic loci. The results of these experiments indicate that the cHS4 insulator, as well as the S/MAR-EW sequences, mediates transcriptional augmentation effects by shielding against repressive effects at the integration loci. These conclusions were originally derived from the excision experiments presented in the first part of our work (Fig. 1), which confirm the observation by Festenstein and colleagues (18) that most (but not all) genomic

sites repress the expression of transgenes. These conclusions were then refined by the cassette exchange procedure, enabling the comparison of multiple element combinations at a number of integration sites. The RMCE principle on which these studies are based rules out any targeting action of particular DNA boundaries, due to the obligatory insertion into predefined genomic loci. Thereby, this strategy overcomes the ambiguity of standard transfection experiments in which insulator constructs might occupy a set of genomic sites, which are different from the (possibly more random) sites at which the naked controls become integrated.

Performance of S/MAR elements and insulators at pre-defined genomic loci. RMCE permitted a detailed comparison between the expression profiles of a reporter gene flanked either by two insulator elements or by two S/MARs. At a moderately expressed locus (N40), cassettes F3HSLGHF and F3ESLGWF both showed transcriptional augmentation relative to a neutral control (F3LSLGLF), as expected for insulators. All subclones showed similar expression levels, arguing against position effect variegation. While there were some fluctuations of expression levels over 26 passages of culture, there were no indications for a consistent long-term shutoff.

The situation seems to be different for a set of S/MAR-like sequences (ISs): a cautious correlation of the data shown in Fig. 3C and Table 1 indicates that IS elements do not act as barriers. Nevertheless, they lead to transcriptional augmentation for individual subclones, which is also reflected by standard deviations between the different subclone populations (Table 1). The augmentation mediated by the IS sequences occurs randomly and is subject to silencing events (Fig. 4). These observations were anticipated by standard stable expression experiments in which a luciferase reporter was provided with an IS element at a position 5' from the promoter. Depending on its presence, we could observe an augmentation effect that varied greatly throughout the population (data not shown). The function of these newly identified intergenic S/MAR sequences with respect to genome organization or transcriptional regulation is still unclear. Eukaryotic genomes have probably arisen from ancient fusions of DNA blocks with unit length. This has been concluded from the existence of repetitive features such as bent sites, which are still apparent in regions without regulatory or coding functions (46). The IS S/MARs presented in this work are located in an extended intergenic region where they occur at approximately 3,000-bp intervals (24). Sites of this nature are unlikely to have immediate regulatory functions but rather appear as ancient signatures of higher chromatin-packaging levels. If these packaging steps depend on an attachment to a supporting structure, this could mediate a barrier function analogous to that of prototype S/MARs (EW) or insulators (11, 19). However, according to our data, this does not seem to be the case.

Data for all five integration sites (Fig. 2) have been compiled in Table 1. Here, we demonstrate that the expression characteristics of the targeted loci are strictly maintained in case of the lambda control (F3LSLGLF), even in the absence of selection pressure. These data can serve the further characterization of the targeted loci, since these spacers of supposedly neutral DNA do not act as insulators. If we combine the information from Fig. 2 with the data from these lambda controls (Table 1), it can clearly be seen that most integration sites

have a repressive transcriptional effect, as was anticipated from the results shown in Fig. 1B. In this group of clones, there is only a single site (N1) that is not improved by the presence of bordering elements, demonstrating that cHS4, S/MARs E and W, and IS elements exert insulating rather than enhancer-like actions, although to different extents. By definition, insulators should normalize negative as well as positive effects from the surroundings. Although the latter effect appears rare, indications for its existence were found for two out of six clones (Fig. 1).

For four of the sites (N40, N7, N33, and N1) S/MARs provided a close-to-perfect insulation. For the same sites, the cHS4 insulator yielded a slightly higher variation, but its effect was also evident at the fifth site (N15), which in its native state mediates the lowest expression levels. This difference in insulation potential hints at different functionalities of these two classes of boundary elements.

S/MARs and cHS4-binding modes. If a neutral sequence integrates close to a matrix attachment site, the interaction between the endogenous chromatin and its nuclear matrix binding partners remains unperturbed. According to the model of Heng and colleagues (10, 27), the presence of S/MAR elements in the construct is expected to strengthen these interactions; this is essentially what we find in the results shown in Fig. 5.

In case of cHS4, the situation is clearly more complex. According to halo-FISH analyses, the integration of cHS4 insulator sequences apparently diminishes the average nuclear matrix association frequency. Yusufzai and colleagues have identified a CTCF-interacting factor, nucleophosmin (B23-numatrin) (51), by which cHS4 constructs become tethered to the surface of nucleoli. While nucleophosmin localizes to the granular portion of the nucleolus to a large extent, parts are also accessible from the exterior in accord with its transport functions. If such a contact is required for at least some actions of cHS4, a scenario arises in which the association partner decides the mode by which it acts as an insulator: if CTCF is its binding partner, it will be tethered to the nucleolar surface, where it may exert enhancer-blocking functions. Although nucleophosmin has been described as a nuclear matrix protein, its interaction with CTCF seems to only partly resist a high-salt or detergent treatment (Fig. 6). These results are also confirmed by Dunn and colleagues, who showed that a minimum of 21.2% of the major 155-kDa CTCF isoform is associated with the nuclear matrix (16). This is consistent with our findings of rare CTCF patches that resist 2 M NaCl in a position close to nucleoli (Fig. 6).

Although the statement by Yusufzai and Felsenfeld that "CTCF and the insulator it binds may be different from usual components of the nuclear matrix" (50) agrees with our conclusions, there appear to be certain discrepancies regarding the experimental evidence. Our observation that the cHS4 insulator is partly released from nuclear matrix (Fig. 5 and Table 2) is unexpected in the light of findings according to which this element acts as a CTCF-dependent nuclear matrix-associated unit. They are in line, however, with previous statements in the literature (13) and with our own *in vitro* reassociation data, which demonstrate that the affinity of cHS4 for the nuclear matrix resembles a negative control rather than an S/MAR standard (Fig. 7). For cHS4, the enhancer-blocking and repres-

barrier activities have been mapped to distinct subdomains of a DNase I-hypersensitive core, and it has been shown that barrier functions of the type observed in our present work do not involve the footprint that was initially assigned to CTCF (40).

It appears conceivable, therefore, that in the case of cHS4 a bordering function is achieved by an alternative mechanism, in a way reminiscent of the human apolipoprotein B intestinal domain which relies on both prototype S/MARs and an insulator: while the 3' S/MAR serves the role of an insulator, an additional CTCF site next to the 5' boundary is required to provide insulation. It has been implied that mutual interactions between these elements explain alternative domain structures in liver and intestine (2).

A possible recent model that comes to mind to explain the particular function of cHS4 elements is based on the active chromatin hub concept, according to which active genes physically interact in the nuclear space with multiple *cis*-regulatory elements causing inactive genes to loop out. Palstra and colleagues (38) have actually shown that the human β -globin HS4-HS5 insulator fragment interacts with other hypersensitive sites within the locus that all bind CTCF. This interaction might be the basis of a nuclear compartment dedicated to RNA polymerase II transcription and thereby an alternative explanation for insulators functioning as boundary elements.

We have stated in the introduction that this study addresses only one out of two activities that have been assigned to insulators, i.e., their bordering function. Current experiments are devoted to its alternative action as enhancer-blocking elements. In the case of the S/MARs, we have to expect another level of complexity, since the action of these elements is highly context dependent (42).

In this study, we have undertaken the first genetic approach to directly compare different classes of bordering elements in an identical chromatin background. Regarding the diversity of effects, synergistic or antagonistic, our results suggest that specific targeting of characterized genomic sites is the prerequisite for solving the major remaining questions associated with the performance of putative chromatin minidomains.

ACKNOWLEDGMENTS

We gratefully acknowledge the cooperation of Prashanth Ak (UC Davis Genome Center) for performing the SIDD analysis and for his continuing interest.

This work was supported by grants from the Deutsche Forschungsgemeinschaft (BO 419-6), BMBF (DHGP I/II), and INTAS (011-0279).

REFERENCES

1. Agarwal, M., T. W. Austin, F. Morel, J. Chen, E. Böhnlein, and I. Plavec. 1998. Scaffold attachment region-mediated enhancement of retroviral vector expression in primary T cells. *J. Virol.* **72**:3720–3728.
2. Antes, T. J., S. J. Namicu, R. E. K. Fournier, and B. Levy-Wilson. 2001. The 5' boundary of the human apolipoprotein B chromatin domain in intestinal cells. *Biochemistry* **40**:6731–6742.
3. Auten, J., M. Agarwal, J. Chen, R. Sutton, and I. Plavec. 1999. Effect of scaffold attachment region on transgene expression in retrovirus vector-transduced primary T cells and macrophages. *Hum. Gene Ther.* **10**:1389–1399.
4. Baer, A., D. Schuebeler, and J. Bode. 2000. Transcriptional properties of genomic transgene integration sites marked by electroporation or retroviral infection. *Biochemistry* **39**:7041–7049.
5. Baer, A., and J. Bode. 2001. Coping with kinetic and thermodynamic barriers: RMCE, an efficient strategy for the targeted integration of transgenes. *Curr. Opin. Biotech.* **12**:473–480.
6. Bell, A. C., and G. Felsenfeld. 2000. Methylation of a CTCF-dependent boundary controls imprinted expression of the *Igf2* gene. *Nature* **405**:482–485.
7. Benham, C., T. Kohwi-Shigematsu, and J. Bode. 1997. Stress-induced duplex DNA destabilization in scaffold/matrix attachment regions. *J. Mol. Biol.* **272**:181–196.
8. Bode, J., C. Benham, A. Knopp, and C. Mielke. 2000. Transcriptional augmentation: modulation of gene expression by scaffold/matrix attached regions (S/MAR elements). *Crit. Rev. Eukaryot. Gene Expr.* **10**:73–90.
9. Bode, J., J. Schlake, M. Iber, D. Schübeler, J. Seibler, E. Snezhkov, and L. Nikolaev. 2000. The transgeneticist's toolbox: novel methods for the targeted modification of eukaryotic genomes. *Biol. Chem.* **381**:801–813.
10. Bode, J., S. Goetze, H. Heng, S. A. Krawetz, and C. Benham. 2003. From DNA structure to gene expression: mediators of nuclear compartmentalization and dynamics. *Chromosome Res.* **11**:435–445.
11. Byrd, K., and V. G. Corces. 2003. Visualization of chromatin domains created by the gypsy insulator of *Drosophila*. *J. Cell Biol.* **162**:565–574.
12. Cesari, F., V. Rennekampff, K. Vintersten, L. G. Vuong, J. Seibler, J. Bode, F. F. Wiebel, and A. Nordheim. 2004. Elk-1 knock-out mice engineered by Flp recombinase-mediated cassette exchange. *Genesis* **38**:87–92.
13. Chung, J. H., M. Whiteley, and G. Felsenfeld. 1993. A 5' element of the chicken beta-globin domain serves as an insulator in human erythroid cells and protects against position effect in *Drosophila*. *Cell* **74**:505–514.
14. Cockerill, P. N., and W. T. Garrard. 1986. Chromosomal loop anchorage of the kappa immunoglobulin gene occurs next to the enhancer in a region containing topoisomerase II sites. *Cell* **44**:273–282.
15. Dobрева, G., J. Dambacher, and R. Grosschedl. 2003. SUMO modification of a novel MAR-binding protein, SATB2, regulates immunoglobulin expression. *Genes Dev.* **17**:3048–3061.
16. Dunn, K. L., H. Zhao, and J. R. Davie. 2003. The insulator binding protein CTCF associates with the nuclear matrix. *Exp. Cell Res.* **288**:218–223.
17. Emery, D. W., M. Aker, and G. Stamatoyannopoulos. 2003. Chromatin insulators and position effects, p. 551–572. *In* S. C. Makrides (ed.), *Gene transfer and expression in mammalian cells*. Elsevier/North-Holland, Amsterdam, The Netherlands.
18. Festenstein, R., M. Tolaini, P. Corbella, C. Mamalaki, J. Parrington, M. Fox, A. Miliou, M. Jones, and D. Kioussis. 1996. Locus control region function and heterochromatin-induced position effect variegation. *Science* **271**:1123–1125.
19. Filippova, G. N., S. Fagerlie, E. M. Klenova, C. Myers, Y. Dehner, G. Goodwin, P. E. Neiman, S. J. Collins, and V. V. Lobanenko. 1996. An exceptionally conserved transcriptional repressor, CTCF, employs different combinations of zinc fingers to bind diverged promoter sequences of avian and mammalian *c-myc* oncogenes. *Mol. Cell Biol.* **16**:2802–2813.
20. Friedrich, G., and P. Soriano. 1991. Promoter traps in embryonic stem cells: a genetic screen to identify and mutate developmental genes in mice. *Genes Dev.* **5**:1513–1523.
21. Garrick, D., S. Fiering, D. I. K. Martin, and E. Whitelaw. 1998. Repeat-induced gene silencing in mammals. *Nat. Genet.* **18**:56–59.
22. Gerasimova, T. L., K. Byrd, and V. G. Corces. 2000. A chromatin insulator determines the nuclear localization of DNA. *Mol. Cell* **6**:1025–1035.
23. Gerdes, M. G., K. C. Carter, P. T. Moen, Jr., and J. B. Lawrence. 1994. Dynamic changes in the higher-level chromatin organization of specific sequences revealed by in situ hybridization to nuclear halos. *J. Cell Biol.* **126**:289–304.
24. Goetze, S., A. Gluch, C. Benham, and J. Bode. 2003. Computational and in vitro analysis of destabilized DNA regions in the interferon gene cluster: potential of predicting functional gene domains. *Biochemistry* **42**:154–166.
25. Goetze, S., Y. Huesemann, A. Baer, and J. Bode. 2003. Functional characterization of transgene integration patterns by halo-FISH: electroporation versus retroviral infection. *Biochemistry* **42**:7035–7043.
26. Gohring, F., and F. O. Fackelmayer. 1997. The scaffold/matrix attachment region binding protein hnRNP-U (SAF-A) is directly bound to chromosomal DNA in vivo: A chemical cross-linking study. *Biochemistry* **36**:8276–8283.
27. Heng, H. H. Q., S. Goetze, C. J. Ye, W. Lu, G. Liu, S. Bremer, M. Hughes, J. Bode, and S. A. Krawetz. 2004. Dynamic features of scaffold/matrix attached regions (S/MARs) in anchoring chromatin loops. *J. Cell Sci.* **117**:999–1008.
28. Hug, B. A., R. L. Wesselschmidt, S. Fiering, M. A. Bender, E. Epner, M. Groudine, and T. J. Ley. 1996. Analysis of mice containing a targeted deletion of β -globin locus control region 5' hypersensitive site 3. *Mol. Cell Biol.* **16**:2906–2912.
29. Iber, M., D. Schübeler, J. Seibler, M. Höxter, and J. Bode. 1999. Efficient FACS selection procedure for cells undergoing Flp-mediated site-specific conversions. [Online.] <http://juergenbode.gmxhome.de/t01668.htm>.
30. Ishii, K., and U. K. Laemmli. 2003. Structural and dynamic functions establish chromatin domains. *Mol. Cell* **11**:237–248.
31. Kay, V., and J. Bode. 1995. Detection of scaffold-attached regions (SARs) by in vitro techniques; activities of these elements in vivo, p. 186–194. *In* A. G. Papavassiliou and S. L. King (ed.), *Methods in molecular and cellular biology 5: methods for studying DNA-protein interactions*. Wiley-Liss, Inc., New York, N.Y.

32. Kirillov, A., B. Kistler, R. Mostoslavsky, H. Cedar, T. Wirth, and Y. Bergman. 1996. A role for nuclear NF- κ B in B-cell-specific demethylation of the Igk locus. *Nat. Genet.* **13**:435–441.
33. Kohwi-Shigematsu, T., K. Maaß, and J. Bode. 1997. A thymocyte factor, SATB1, suppresses transcription of stably integrated MAR-linked reporter genes. *Biochemistry* **36**:12005–12010.
34. Kowalski, D., D. A. Natale, and M. J. Eddy. 1988. Stable DNA unwinding, not “breathing,” accounts for single-strand-specific nuclease hypersensitivity of specific A+T-rich sequences. *Proc. Natl. Acad. Sci. USA* **85**:9464–9468.
35. Mielke, C., Y. Kohwi, T. Kohwi-Shigematsu, and J. Bode. 1990. Hierarchical binding of DNA fragments derived from scaffold-attached regions: correlation of properties in vitro and function in vivo. *Biochemistry* **29**:7475–7485.
36. Mirkovitch, J., M. E. Mirault, and U. K. Laemmli. 1984. Organization of the higher-order chromatin loop: specific DNA attachment sites on nuclear scaffold. *Cell* **39**:223–232.
37. Nabirochkin, S., M. Ossokina, and T. Heidmann. 1998. A nuclear matrix/scaffold attachment region co-localizes with the gypsy retrotransposon insulator sequence. *J. Biol. Chem.* **273**:2473–2479.
38. Palstra, R. J., B. Tolhuis, E. Splinter, R. Nijmeijer, F. Grosveld, and W. deLaat. 2003. The beta-globin nuclear compartment in development and erythroid differentiation. *Nat. Genet.* **35**:190–194.
39. Raetsch, A., S. Joos, P. Kioschis, and P. Lichter. 2002. Topological organization of the MYC/IGK locus in Burkitt’s lymphoma cells. *Exp. Cell Res.* **273**:12–20.
40. Recillas-Targa, F., M. J. Pikaart, B. Burgess-Beusse, A. C. Bell, M. D. Litt, A. G. West, M. Gaszner, and G. Felsenfeld. 2002. Position-effect protection and enhancer blocking by the chicken beta-globin insulator are separable activities. *Proc. Natl. Acad. Sci. USA* **99**:6883–6888.
41. Schlake, T., D. Klehr-Wirth, M. Yoshida, T. Beppu, and J. Bode. 1994. Gene expression within a chromatin domain: the role of core histone hyperacetylation. *Biochemistry* **33**:4197–4206.
42. Schübeler, D., C. Mielke, K. Maaß, and J. Bode. 1996. Scaffold/matrix-attached regions act upon transcription in a context-dependent manner. *Biochemistry* **35**:11160–11169.
43. Seibler, J., D. Schübeler, S. Fiering, M. Groudine, and J. Bode. 1998. DNA cassette exchange mediated by FLP recombinase: an efficient strategy for the repeated modification of tagged loci by marker-free constructs. *Biochemistry* **37**:6229–6234.
44. Singh, G. B., J. A. Kramer, and S. A. Krawetz. 1997. Mathematical model to predict regions of chromatin attachment to the nuclear matrix. *Nucleic Acids Res.* **25**:1419–1425.
45. Taniguchi, M., M. Sanbo, S. Watanabe, I. Naruse, M. Mishina, and T. Yagi. 1998. Efficient production of Cre-mediated site-directed recombinants through the utilization of the puromycin resistance gene, *pac*: transient gene-integration marker for ES cells. *Nucleic Acids Res.* **26**:679–680.
46. Trifonov, E. N., A. Kirzhner, M. V. Kirzhner, and I. N. Berezovsky. 2001. Distinct stages of protein evolution as suggested by protein sequence analysis. *J. Mol. Evol.* **53**:394–401.
47. Tsutsui, K. 1998. Synthetic concatemers as artificial MAR: importance of a particular configuration of short AT-tracts for protein recognition. *Gene Ther. Mol. Biol.* **1**:581–590.
48. West, A. G., M. Gaszner, and G. Felsenfeld. 2002. Insulators: many functions, many mechanisms. *Genes Dev.* **16**:271–288.
49. Xu, Q., Li, M., Adams, J., and H. N. Cai. 2004. Nuclear location of a chromatin insulator in *Drosophila melanogaster*. *J. Cell Sci.* **117**:1025–1032.
50. Yusufzai, T. M., and G. Felsenfeld. 2004. The 5’-HS4 chicken beta-globin insulator is a CTCF-dependent nuclear matrix-associated element. *Proc. Natl. Acad. Sci. USA* **101**:8620–8624.
51. Yusufzai, T. M., H. Tagami, Y. Nakatani, and G. Felsenfeld. 2004. CTCF tethers an insulator to subnuclear sites, suggesting shared insulator mechanisms across species. *Mol. Cell* **13**:291–298.